

NON-DETECTION OF THE PUTATIVE SUBSTELLAR COMPANION TO HD 149382

JACKSON M. NORRIS¹, JASON T. WRIGHT¹, RICHARD A. WADE, SUVRATH MAHADEVAN¹, SARA GETTEL¹
 Department of Astronomy and Astrophysics, 525 Davey Lab, The Pennsylvania State University, University Park, PA 16802
 ACCEPTED TO APJ: September 29, 2011

ABSTRACT

It has been argued that a substellar companion may significantly influence the evolution of the progenitors of sdB stars. Recently, the bright sdB star HD 149382 has been claimed to host a substellar (possibly planetary) companion with a period of 2.391 days. This has important implications for the evolution of the progenitors of sdB stars as well as the source of the UV-excess seen in elliptical galaxies. In order to verify this putative planet, we made 10 radial velocity measurements of HD 149382 over 17 days with the High Resolution Spectrograph at the Hobby-Eberly Telescope. Our data conclusively demonstrate that the putative substellar companion does not exist, and they exclude the presence of almost any substellar companion with $P < 28$ days and $M \sin i \gtrsim 1 M_{\text{Jup}}$.

Subject headings: binaries: close - binaries: spectroscopic - planetary systems - stars: horizontal-branch - stars: individual (HD 149382) - subdwarfs

1. INTRODUCTION

The nature of the progenitors of subdwarf B (sdB) stars is not well understood. One theoretical formation method is through a common-envelope (CE) phase of evolution with an orbital companion (Han et al. 2002, 2003). As the progenitor star ascends the first red giant branch, interaction with a companion via a CE may cause it to lose large amounts of mass. When the progenitor star finally ignites core helium burning on the horizontal branch, it has a small radius, a high effective temperature, and a low-mass hydrogen envelope that cannot sustain shell burning: it is a sdB star. Soker (1998) suggests that a substellar companion (a brown dwarf or planet) may be massive enough to survive this CE phase without merging with the host star. This implies that some sdBs may be created via the evolution of single stars with large planetary companions. In addition to their importance as tracers of the many paths of stellar evolution, sdB stars have broader importance in that they may be the dominant source of the UV-excess seen in elliptical galaxies (Brown et al. 1997, 2008).

HD 149382 is the brightest known sdB star, and thus provides an excellent opportunity to better understand the progenitors of sdB stars. It is an sdOB star with atmospheric parameters $T_{\text{eff}} = 35500 \pm 500$ K, $\log g = 5.80 \pm 0.05$ (Geier et al. 2009, hereinafter G09), and a pattern of photospheric abundances altered by diffusion processes (Baschek et al. 1982, who found $T_{\text{eff}} = 35000 \pm 2000$ K, $\log g = 5.5 \pm 0.3$). G09 claim to have detected a substellar companion to HD 149382 with a mass of $8 - 23 M_{\text{Jup}}$ using 16 radial velocity (RV) measurements collected from four different telescopes over a span of four years. G09 claim this is significant because it suggests that the progenitors of sdB stars can be stripped of their hydrogen envelopes by substellar companions during the CE phase, strongly supporting Soker (1998). This is the first claim of a close substellar companion to an sdB star able to affect the evolution of its host. For brevity we will

use the word “planet” to refer to a substellar companion of HD 149382, whether a true planet or a brown dwarf.

Jacobs et al. (2011) reported a non-detection of the claimed planet from their own RV measurements of HD 149382 using the HERMES spectrograph (Raskin et al. 2011). Their upper limit on the RV variability of HD 149382 was 0.8 km s^{-1} , nearly three times lower than the amplitude reported by G09. Since a planet with the reported short orbital period would have important implications, we independently sought verification of its existence, as we describe here.

2. DATA

We observed HD 149382 on 10 nights between April 10-27, 2010 using the High Resolution Spectrograph (HRS; Tull 1998) in its $R = 60,000$ configuration, at the Hobby-Eberly Telescope (HET; Ramsey et al. 1998), a 9.2m telescope stationed at the McDonald Observatory near Fort Davis, Texas. We exploited the queue scheduling of this telescope (Shetrone et al. 2007) to efficiently make our 10 observations and acquire good phase coverage of the orbit. Typical single-exposure signal-to-noise ratios at blaze peak near 5500 \AA were 100 per 4-pixel resolution element. The use of a single, fiber-fed spectrograph should reduce the potentially significant systematic velocity errors that G09 may have incurred combining measurements made from four different telescopes.

Our observing procedure was to obtain two exposures of the star through the $2''$ fiber followed immediately by two exposures with the iodine absorption cell inserted in the beam. The cell served to measure night-to-night instrumental offsets due to imperfect repeatability of the instrument configuration. We also obtained bracketing thorium-argon (ThAr) lamp exposures through the calibration fiber, and the standard ThAr exposures and flat lamp exposures through the iodine cell at the beginning or end of each night. On the first night, we obtained only one stellar exposure of each type, and on the final night we obtained three.

2.1. Reducing Spectra

¹ Center for Exoplanets and Habitable Worlds, 525 Davey Lab, The Pennsylvania State University, University Park, PA 16802

The spectra were reduced using **REDUCE**, an advanced image reduction package designed to reduce 2-dimensional, raw echelle spectra into 1-dimensional, wavelength-calibrated spectra (Piskunov & Valenti 2002). The reduction was modified slightly to accommodate fiber-fed spectra, rather than slit spectra. Each observation contains information on two charge-coupled devices (CCDs), a “blue” CCD and a “red” CCD; we limited our analysis to the blue CCD, where we expect most velocity information to be located. We extracted 47 orders of 1-dimensional spectra from the blue CCD.

When determining velocities, we stacked all stellar exposures from the same night into a single spectrum. The time between stellar exposures on the same night is always less than 31 minutes; finding RV from a stacked spectrum for each night should not change our results, since any change in the RV of the star will be small over the “smoothing interval” of our exposures. Since we combined pure stellar exposures with stellar-plus-iodine-cell exposures, we were careful to analyze only those orders that contain no iodine lines.

2.2. Visual Companion

In addition to the putative substellar companion, HD 149382 features a known visual, stellar companion. Østensen et al. (2005) detected this visual companion using adaptive optics. The visual companion is about $1''$ away (corresponding to 75 AU, Jacobs et al. 2011) while the HRS fiber diameter is $2''$, so we likely collected light from both stars. We therefore took care in our velocity analysis to select only lines expected from the primary. Ulla & Thejll (1998) detected an infrared excess in HD 149382, probably due to this visual companion, but Geier et al. (2010) detect no spectral features from the companion in the optical. Since we also observed in the optical, and since any orbital motion between the stars must be too slow to be detectable over a 17 day span, we do not expect significant RV errors due to the companion spectrum.

3. METHOD

3.1. Line Selection

To aid in selecting absorption lines that are unequivocally from the primary star, and not from the faint companion, we generated a synthetic spectrum from a Castelli & Kurucz model² (Castelli & Kurucz 2003) with the approximate parameters of HD 149382, as reported by G09. We started from a solar-abundance Kurucz atmosphere model in LTE with $T_{\text{eff}} = 35000$ K, $\log g = 5.0$.

We selected a line list from the Vienna Atomic Line Database (VALD; Kupka et al. 2000) spanning the wavelength range 415 – 500 nm, and corresponding to the model selected. We used the **SYNTH3** code (Kochukhov 2007) to generate a stellar spectrum, adopting abundances for elements derived by Baschek et al. (1982), and solar abundances of Asplund et al. (2009) for remaining elements. The resulting spectrum was broadened with a rotational profile of ($v \sin i = 2.4 \text{ km s}^{-1}$), and convolved with a Gaussian profile to match the $R = 60,000$ HRS observation.

The synthetic spectrum is not an exact match to the observed spectrum of HD 149382, as several lines are

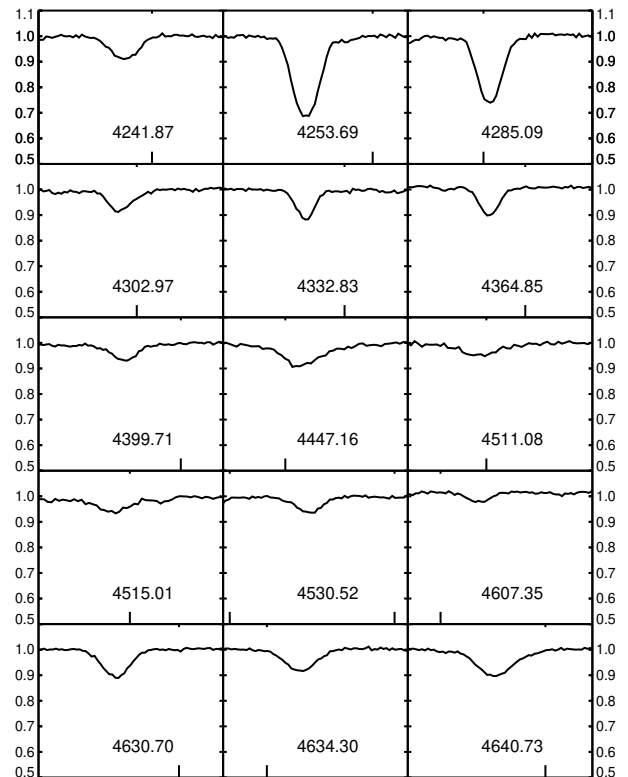


FIG. 1.— An atlas illustrating the 15 lines used in this RV analysis. Each plot presents a region of the spectrum centered on the indicated wavelength (listed in Å) averaged over all observations. The span of the x-axis in each plot is given in Table 1. The tick marks on the x-axes represent integer air wavelengths in Å.

present in the model but not the data (and vice versa). We note though, that such an exact match is not required for our purpose. The synthetic spectrum is of sufficient fidelity to unambiguously identify lines that belong to the primary star, and we chose these lines (i.e. present in the model *and* the data) to measure the RVs.

We visually selected 15 regions containing moderately deep and narrow metal absorption features. Each of these 15 pixel groups contains one or more lines at wavelengths predicted from the model. Our final selection of absorption features is given in Table 1, and the averaged observed spectrum for each pixel group is shown in Figure 1.

3.2. Radial Velocity Determination

A potential source of systematic error is the stability of the HRS wavelength solution. We checked our ability to determine precise wavelength solutions on different nights by comparing the night-to-night shift in the wavelength solution to the shifts we measured in the iodine region of the stellar spectra. Since the iodine exposures were made through the science fiber and have extremely high Doppler content, they provide a highly sensitive measurement of any instrumental drift affecting stellar velocity measurements. We compared the shifts measured in 192 63-pixel sections of the iodine region (through a cross-correlation analysis in pixel space) to the shifts we measured in the same sections using the nearest adjacent ThAr exposures (made through the calibration fiber). On each night, the median shift

² See <http://kurucz.harvard.edu>

TABLE 1
ABSORPTION FEATURES USED FOR RV MEASUREMENT

Min. λ [Å] (air)	Max. λ [Å] (air)	Median λ [Å] (air)	Species	Lines
4241.33	4242.42	4241.87	N II	2
4253.19	4254.19	4253.69	Fe III, S III, O II	5
4284.59	4285.59	4285.09	Ca III, S III, O II	3
4302.42	4303.51	4302.97	Ca III, O II	3
4332.27	4333.38	4332.83	S III, O II, N III	3
4364.30	4365.40	4364.85	S III	1
4399.16	4400.25	4399.71	Ca III, Zn III	2
4446.67	4447.65	4447.16	N II	1
4510.57	4511.58	4511.08	N III, Ne II	4
4514.52	4515.49	4515.01	N III, Ne II, C III	3
4529.96	4531.08	4530.52	N II, N III	2
4606.81	4607.88	4607.35	Ne II, N II	2
4630.11	4631.28	4630.70	N II, O III, Si IV	5
4633.73	4634.87	4634.30	N III, Ne II	2
4640.18	4641.28	4640.73	N III	1

NOTE. — The absorption features predicted from our synthetic spectrum in our 15 pixel groups. Only the lines whose flux minima occur within the search area are included in the tabulation of species and number of lines.

measured from all 192 sections differs by $\lesssim 0.1$ pixel between the ThAr exposures and the iodine region of the stellar spectra, indicating that the ThAr exposures track the instrumental shifts of the basement-mounted, temperature-controlled HRS as observed through the science fiber to better than $\sim 100 \text{ m s}^{-1}$. The stability of the wavelength solution (i.e., its night-to-night precision) is not a limiting factor in our RV precision.

To determine a RV for each night’s average spectrum, we rebinned our model spectrum into the wavelengths of each pixel group, using the wavelength solution determined from the adjacent ThAr exposures. We then calculated the peak in the cross-correlation function (CCF) in pixel space between our model and our observation, and used the dispersion of the wavelength solution to calculate a velocity shift. The primary source of uncertainty in our RV measurements is the uncertainty in the location of the CCF peak due to the finite signal-to-noise ratio of the data.

Each of the 15 pixel groups yielded its own set of RV measurements. We subtracted the barycentric motion of the telescope using routines provided by the California Planet Survey, which are proven below 0.001 km s^{-1} (e.g. Howard et al. 2010). Over the timespan of our data, the change in barycentric correction amounts to almost 7 km s^{-1} . Probably because of line blends, the CCFs for the different regions yield RVs that do not share a common apparent systemic velocity, although they independently detect the barycentric motion. Since we are primarily concerned with the acceleration of the star in its putative orbit rather than the systemic velocity of the star, we subtracted the mean RV of each pixel group from its time series. For each night, we then averaged the resulting differential RVs derived from each pixel group. We used the standard error of the mean of the relative RVs to determine the “internal” error on each night’s measurement. Our RVs thus have an arbitrary zero point. We present our results after applying these corrections in Table 2.

4. RESULTS

TABLE 2
RADIAL VELOCITIES

Barycentric Julian Date [-2455000 days]	Velocity [km/s]
296.924	-0.06 ± 0.12
298.915	0.01 ± 0.06
302.906	-0.13 ± 0.07
305.898	-0.02 ± 0.06
307.878	0.23 ± 0.10
308.884	0.17 ± 0.15
309.896	-0.24 ± 0.15
311.876	0.10 ± 0.10
312.884	-0.05 ± 0.09
313.900	0.07 ± 0.15

The root-mean-square variation of our measured velocities is 0.13 km s^{-1} . The (reduced) χ^2_ν value for the null hypothesis of no measured stellar acceleration is 1.61, suggesting that either our uncertainties are slight underestimates or that the target is intrinsically variable at this level.

To verify that these measurements are inconsistent with the claim of G09, we fitted our RVs to a circular Keplerian model using the RVLIN code (Wright & Howard 2009), with an initial period estimate equal to the value quoted by G09. Because we are testing a specific hypothesis, we limited the solutions to values within 5-sigma of the values quoted by G09, specifically $P = \{2.381, 2.401\}$ days. We allowed all other orbital elements in the fit to float, including the phase, since the time elapsed since the G09 measurements is sufficiently long that the propagated phase is uncertain.

Our best fit results are period $P = 2.401$ days and RV semi-amplitude $K = 0.05 \text{ km s}^{-1}$ (Fig. 2). This semi-amplitude is much smaller than the claim of $2.3 \pm 0.1 \text{ km s}^{-1}$ by G09, and the difference lies well outside the uncertainties of the two measurements. We also fitted our data to a sinusoid with exactly the semi-amplitude and period reported by G09, but with unknown phase and zero point offset, using the IDL routine `mpfitfun` (Markwardt 2009). Figure 3 demonstrates the discrepancy between our findings and those of G09. Broadening our search beyond a 5-sigma window around the putative period, we find that other best fit values for K for all similarly short periods are below our RV errors (Fig. 4, Table 2) indicating that they are consistent with 0 km s^{-1} .

Because some pixel groups contain weaker lines than other groups, we repeat our analysis for subsets of the groups that omit the poorest features (e.g. omit groups 9 and 12 in Table 1). Our results do not change significantly for multiple subsets, indicating that our exact selection of lines is not important. Furthermore, as Figure 3 indicates, since the absolute value of all the RVs in our pixel groups are well underneath the semi-amplitude found by G09, it is unlikely that any combination of pixel groups will provide a similar fit to that found by G09.

We have no reason to suspect the existence of planets at other periods, and our experiment was designed only to confirm or disconfirm this particular claim. Nonetheless, we have thoroughly searched our data for any periodicity to determine the parameter space for planets that is excluded by our data. We restrict our search to

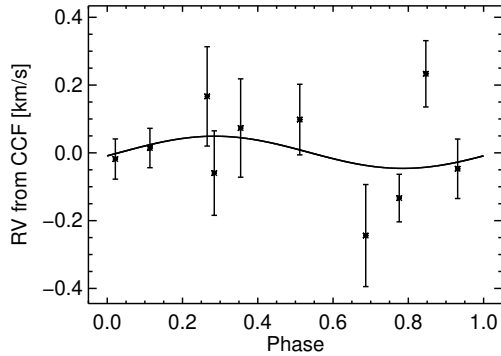


FIG. 2.— Best fitted phase-folded RV curve for HD 149382, limiting the period to a range near the previously reported value (gray area of Fig. 4) while allowing the semi-amplitude and phase to drift. The central value near 0 km s^{-1} does *not* represent the systemic velocity of the star, since we have subtracted the mean values of each line from their nightly values. Our best fit within 5-sigma of the period reported by G09 is $P = 2.401 \text{ d}$ and $K = 0.05 \text{ km s}^{-1}$, which is much less than the putative value of $K = 2.3 \pm 0.1 \text{ km s}^{-1}$.

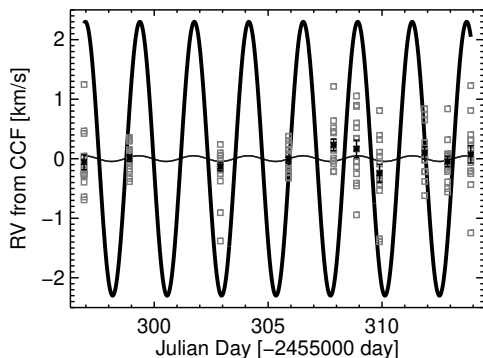


FIG. 3.— The gray boxes show our RV measurements for all 15 absorption features on each night. The black asterisks show the mean of each night’s measurements and the associated standard error of the mean. The thin line shows our best fit within a 5-sigma range of P near value reported by G09 (gray area of Fig. 4). The thick line shows the sinusoid reported by G09. As in Fig 2, the central value near 0 km s^{-1} does *not* represent the systemic velocity of the star.

periods between 0.2–28 days, limited both by a semimajor axis $\gtrsim 1$ stellar radius as well as the longest period easily detectable with our data span. We further restrict our search to circular orbits.

The observational cadence of the HET creates “blind spots” in our coverage near the harmonics of 1 sidereal day. We have excluded these regions from the following analysis (we define such a “blind spot” as any period for which we have no data points for a stretch of phase larger than 144 degrees, or 0.4 cycles, and for some higher harmonics where the data cluster tightly at two phases 180 degrees apart).

We determined the semi-amplitudes of the best fit sinusoids for a well-sampled set of periods between 0.2–28 days. The largest semi-amplitudes we find are near 0.17 km s^{-1} , which we find at a variety of periods across our search space. If we adopt the upper limit of the range of masses of HD 149382 reported by G09 of $0.53 M_{\odot}$, then we can translate these semi-amplitudes into upper

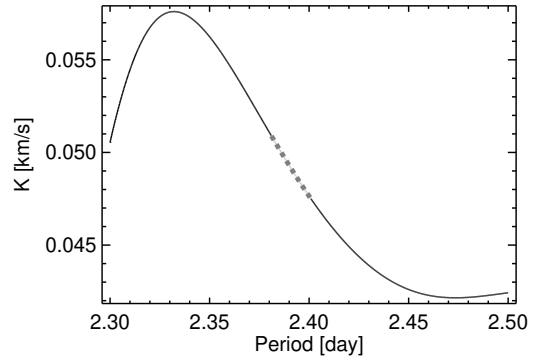


FIG. 4.— Best fit semi-amplitude K as a function of period P . The thick, dotted, gray segment corresponds to a 5-sigma range centered on the period reported by G09, and includes the fit used in Fig. 3. At all points near the putative $2.391 \pm 0.002 \text{ day}$ period, our measured K is much less than the value of $2.3 \pm 0.1 \text{ km s}^{-1}$ reported by G09.

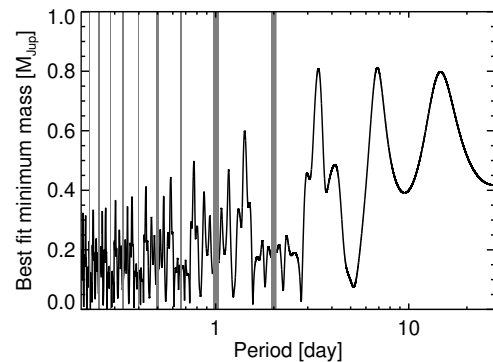


FIG. 5.— Full period-minimum mass diagram for all periods probed in this work. “Blind spots” created by the cadence imposed by the fixed elevation of the HET are shaded in gray; in these regions our phase coverage is too poor to put meaningful constraints on the presence of RV companions. Minimum masses correspond to the $M \sin i$ values for planets in circular orbits at the given period with the amplitude of the best-fit sinusoid to our data at each period.

limits on the minimum companion masses ($M \sin i$) at each trial period. We find no best-fit companions with $M \sin i$ in excess of $0.8 M_{\text{Jup}}$, which makes the existence of any close-in giant planet with $M \sin i \gtrsim 1 M_{\text{Jup}}$ highly unlikely. Figure 5 illustrates our upper limits and blind spots. In principle, a more massive companion could exist in a face-on orbit, or in one of our period blind spots (or perhaps in a highly eccentric orbit), but this remaining parameter space is extremely narrow.

Our results agree with those of Jacobs et al. (2011), who also find no massive planets out to $P = 50$ days through an analysis of four He I lines, although our constraints on the RV variability of HD 149382 are over four times more stringent.

5. DISCUSSION

There are several claims of substellar companions in orbit around hot subdwarf stars, summarized in Schuh (2010). With the exception of HD 149382 and SDSS J08205+0008 (discussed below), these claims are all based on the interpretation of residuals in an $O - C$ diagram, in which observed (“O”) moments of eclipse

or pulsation maximum are compared with a calculated (“ C ”) ephemeris. A quasi-sinusoidal pattern of residuals is interpreted in terms of a light-time effect across the orbit of the subdwarf. For the eclipsing systems, the inferred “planet” is circumbinary; for the case of pulsations (V391 Peg: Silvotti et al. 2007), the sdB star is otherwise thought to be single. Except for HD 149382 and CS 1246 (see below), all of the claimed orbital periods for substellar companions to sdB stars are long, in the range of 3 to 16 years. Nearly always, a parabolic term is fitted to the $O - C$ residuals along with the orbital sinusoid. The parabola represents either an evolving pulsation period or an evolving orbital period of the eclipsing binary, as angular momentum is transferred by tides from the orbit to the binary companion, which undergoes “magnetic braking”. The relatively short observational timespans, with the additional issue of correlations between model parameters describing the parabolic term and the light-time orbit, conspire to make these claims of substellar companions quite fragile — new observations tend to destroy the previous solution. (See Parsons et al. 2010, for examples of broken timing orbits in the case of eclipsing binaries with white dwarf primaries.) Quasi-cyclical variation in $O - C$ residuals for binaries may have causes other than orbital motion involving a third body, such as the “Applegate mechanism” (Applegate 1992), in which mass quadrupole variations induced by stellar activity cycles alter the effective Keplerian mass of the binary.

The only timing-based ($O - C$) detection of a companion to an sdB star that has been confirmed by an RV study is that of CS 1246 (Barlow et al. 2011a,b). Here the orbital period is 14.1 days, but the minimum mass of the companion is $M \sin i \approx 0.13 M_{\odot}$, above the substellar limit.

Some of the claimed substellar companions in long-period orbits may be corroborated with continuing observations, and others will surely be found. It is unlikely, however, that these large orbits tell us anything directly about the formation process of the sdB stars themselves. (Schuh (2010) does discuss the possibility that large orbits may be indicators for the previous existence of inner planets, destroyed in a CE process.) It is also important to bear in mind that only a lower limit $M \sin i$ to the companion mass M is found from these timing solutions.

Short-period orbits of substellar companions around sdB stars are of more interest for elucidating the prior history of the sdB star. In addition to the idea that a planet may assist in removing the hydrogen envelope from the proto-sdB stars (Soker 1998), there is the possibility that “second-generation” planets may form in the debris left from the merger of two helium white dwarfs (the “helium planet” scenario of Silvotti 2008). Note however, that since a merger between a helium white dwarf and a low-mass hydrogen-burning star may also create an sdB star (Clausen & Wade 2011), a resulting second-generation planet need not be of exotic composition.

The formation of sdB stars through envelope stripping by planets is an intriguing hypothesis, but in light of the fact that the claimed planet HD 149382 b does not exist, it currently has little observational support. To date

the only such companion known is that in the eclipsing sdB+brown dwarf system SDSS J08205+0008, found by Geier et al. (2011). The orbital period is 0.096 days, and the estimated mass for the strongly irradiated companion, for reasonable estimates of the mass of the sdB star, is in the range $0.045 - 0.068 M_{\odot}$, slightly below the hydrogen-burning limit. This pushes the lower mass limit for companions in short-period sdB systems to somewhat lower masses than before (see Geier et al. 2011, for discussion of HW Vir systems), but hardly into the planetary realm. Given the potential importance of significantly substellar companions to the understanding of the extremes of binary star evolutionary channels as well as the formation of second-generation planets, searches for such companions to sdB stars in short-period orbits should continue.

Meanwhile, the putative planet orbiting HD 149382 has already been put to use by De Marco et al. (2011) in revising the “ α formalism” for CE binary evolution. Those authors make the CE efficiency parameter α a strongly decreasing function of mass ratio. This conclusion relies strongly on the large value of $\alpha \sim 33$ inferred for the putative HD 149382 “planetary” system. De Marco et al. (2011) recognized HD 149382 as an outlier, and presented parametrized forms for α derived with and without including it in the sample of studied systems. With our demonstration that this system does not exist (at least, as specified by G09), the weaker dependence of α on mass ratio is favored.

6. SUMMARY

Our findings conclusively refute the Geier et al. (2009) claim of a substellar object orbiting the hot subdwarf star HD 149382. The orbital solution found by Geier et al. is strongly inconsistent with our RV measurements. Our best fit results near the putative planet’s best period are $P = 2.401$ days and $K = 0.05 \text{ km s}^{-1}$, which is consistent with 0 km s^{-1} given the uncertainties in our measurements. We can further confidently rule out planets with $M \sin i > 1 M_{\text{Jup}}$ in circular orbits with periods < 28 days, except for a few special cases arising from the cadence of our observations.

We argue that the evolutionary origins of this hot subdwarf cannot involve an extant, close-in companion of giant planet mass or greater.

This work was partially supported by funding from the Center for Exoplanets and Habitable Worlds. The Center for Exoplanets and Habitable Worlds is supported by the Pennsylvania State University, the Eberly College of Science, and the Pennsylvania Space Grant Consortium. R.W. gratefully acknowledges support from National Science Foundation grant AST-0908642.

The Hobby-Eberly Telescope (HET) is a joint project of the University of Texas at Austin, the Pennsylvania State University, Stanford University, Ludwig-Maximilians-Universität München, and Georg-August-Universität Göttingen. The HET is named in honor of its principal benefactors, William P. Hobby and Robert E. Eberly.

REFERENCES

- Applegate, J. H. 1992, *ApJ*, 385, 621
- Asplund, M., Grevesse, N., Sauval, A. J., & Scott, P. 2009, *ARA&A*, 47, 481

- Barlow, B. N., Dunlap, B. H., & Clemens, J. C. 2011a, *ApJ*, 737, L2
- Barlow, B. N., Dunlap, B. H., Clemens, J. C., Reichart, D. E., Ivarsen, K. M., Lacluyze, A. P., Haislip, J. B., & Nysewander, M. C. 2011b, *MNRAS*, 414, 3434
- Baschek, B., Scholz, M., Kudritzki, R. P., & Simon, K. P. 1982, *A&A*, 108, 387
- Brown, T. M., Ferguson, H. C., Davidsen, A. F., & Dorman, B. 1997, *ApJ*, 482, 685
- Brown, T. M., Smith, E., Ferguson, H. C., Sweigart, A. V., Kimble, R. A., & Bowers, C. W. 2008, *ApJ*, 682, 319
- Castelli, F., & Kurucz, R. L. 2003, in *IAU Symposium*, Vol. 210, *Modelling of Stellar Atmospheres*, ed. N. Piskunov, W. W. Weiss, & D. F. Gray, 20P
- Clausen, D., & Wade, R. A. 2011, *ApJ*, 733, L42
- De Marco, O., Passy, J.-C., Moe, M., Herwig, F., Mac Low, M.-M., & Paxton, B. 2011, *MNRAS*, 411, 2277
- Geier, S., Edelmann, H., Heber, U., & Morales-Rueda, L. 2009, *ApJ*, 702, L96
- Geier, S., et al. 2010, *Ap&SS*, 329, 91
- . 2011, *ApJ*, 731, L22
- Han, Z., Podsiadlowski, P., Maxted, P. F. L., & Marsh, T. R. 2003, *MNRAS*, 341, 669
- Han, Z., Podsiadlowski, P., Maxted, P. F. L., Marsh, T. R., & Ivanova, N. 2002, *MNRAS*, 336, 449
- Howard, A. W., et al. 2010, *ApJ*, 721, 1467
- Jacobs, V. A., et al. 2011, in *AIP Conf. Ser.*, Vol. 1331, *Planetary Systems Beyond the Main Sequence*, ed. S. Schuh, H. Drechsel, & U. Heber, 304–309
- Kochukhov, O. P. 2007, in *Physics of Magnetic Stars*, ed. I. I. Romanyuk, D. O. Kudryavtsev, O. M. Neizvestnaya, & V. M. Shapoval, 109
- Kupka, F. G., Ryabchikova, T. A., Piskunov, N. E., Stempels, H. C., & Weiss, W. W. 2000, *Baltic Astronomy*, 9, 590
- Markwardt, C. B. 2009, in *ASP Conf. Ser.*, Vol. 411, *Astronomical Data Analysis Software and Systems XVIII*, ed. D. A. Bohlender, D. Durand, & P. Dowler, 251
- Østensen, R., Heber, U., & Maxted, P. 2005, in *ASP Conf. Ser.*, Vol. 334, *14th European Workshop on White Dwarfs*, ed. D. Koester & S. Moehler, 435
- Parsons, S. G., et al. 2010, *MNRAS*, 407, 2362
- Piskunov, N. E., & Valenti, J. A. 2002, *A&A*, 385, 1095
- Ramsey, L. W., et al. 1998, in *SPIE Conf. Ser.*, Vol. 3352, *Advanced Technology Optical/IR Telescopes VI*, ed. L. M. Stepp, 34
- Raskin, G., et al. 2011, *A&A*, 526, A69
- Schuh, S. 2010, *Astronomische Nachrichten*, 331, 489
- Shetrone, M., et al. 2007, *PASP*, 119, 556
- Silvotti, R. 2008, in *ASP Conf. Ser.*, Vol. 392, *Hot Subdwarf Stars and Related Objects*, ed. U. Heber, C. S. Jeffery, & R. Napiwotzki, 215
- Silvotti, R., et al. 2007, *Nature*, 449, 189
- Soker, N. 1998, *AJ*, 116, 1308
- Tull, R. G. 1998, in *SPIE Conf. Ser.*, Vol. 3355, *Optical Astronomical Instrumentation*, ed. S. D’Odorico, 387
- Ulla, A., & Thejll, P. 1998, *A&AS*, 132, 1
- Wright, J. T., & Howard, A. W. 2009, *ApJS*, 182, 205